IOP Publishing European Journal of Physics
Eur. J. Phys. **41** (2020) 035803 (14pp) https://doi.org/10.1088/1361-6404/ab78a5

Experimental study of the coefficient of rolling friction of the axle of a Maxwell's wheel on a soft horizontal surface

Surajit Chakrabarti[1], **Rajesh B Khaparde**[2] and **Alimohammed H Kachwala**[2]

[1] Ramakrishna Mission Vidyamandira, Belur Math, Howrah, India
[2] Homi Bhabha Centre for Science Education, Tata Institute of Fundamental Research, Mankhurd, Mumbai, India

E-mail: surnamchakrabarti@gmail.com

Received 10 October 2019, revised 22 January 2020
Accepted for publication 21 February 2020
Published 8 April 2020

Abstract

We have studied the rolling motion of a specially designed Maxwell's wheel. The rigid axle of the wheel rolls on a pair of horizontal tracks. The central disc of the wheel rotates in the air symmetrically betweeen the tracks. Soft nitrile foam sheets have been pasted on the metallic tracks. We attach a pair of identical metal sleeves on the axle on two sides which allows us to change the effective rolling diameter of the axle. By this arrangement we can change the ratio of the rotational energy of the wheel over its translational energy. The soft surface undergoes deformation as a result of which the surface reaction force acts at a point on the axle slightly in front of the ideal contact point between the two. This offset distance has been related to the deceleration of the wheel as well as its loss of energy. From the deceleration we determine the offset distance. The coefficient of rolling friction determined from the offset distance shows a power law dependence on the dimensionless energy ratio.

Keywords: rolling friction, Maxwell's wheel, soft surface, coefficient of rolling, energy ratio, power law, offset distance

(Some figures may appear in colour only in the online journal)

1. Introduction

Rolling motion has been a field of intensive study because of its importance in engineering applications. Innumerable experiments have been performed to understand rolling friction. The coefficient of rolling friction turns out to be small compared to static or kinetic friction.

Energy loss is found to be very small for a rigid sphere or a cylinder rolling on a rigid surface. That is why the discovery of wheels has played such an important role in the advancement of human civilization. Considering the simplest case of the rolling of a cylinder on a horizontal surface without force being applied, it is common knowledge that the rolling object undergoes deceleration and loses energy and ultimately comes to rest. Different authors use different expressions for the loss of energy in terms of the coefficient of rolling friction.

It is well accepted that the loss of energy in rolling motion occurs because of the deformation and subsequent reformation of the surface resulting in hysteresis which is responsible for the loss of energy. As a result of the deformation, reaction force of the surface on the rolling object acts at a point which is slightly offset from the centre of the object in the direction of motion. Different authors have used different definitions for the coefficient of rolling friction. The offset distance has been defined as the coefficient of rolling friction in some works [1, 2]. Domenech *et al* [1] have studied the motion of spherical balls rolling over inclined as well as horizontal planes. They have experimentally determined this offset distance for spherical balls of different sizes and materials. In the case of horizontal motion the offset distances have been determined from the deceleration of the balls. Another recent work [3] has studied the energy loss of spherical balls rolling over horizontal surfaces.

In the present work we have studied the horizontal motion of a Maxwell's wheel [4] which has been set with a definite initial velocity by allowing it to come down a pair of inclined planes attached to the horizontal tracks. In our experiment, the axle runs on a horizontal pair of parallel tracks with soft nitrile foam sheet [5] stuck on the tracks. The soft surface increases the loss of energy of the wheel. The disc of the Maxwell's wheel rotates symmetrically in the air between the tracks. A pair of identical metal sleeves can be attached to the axle on two sides. Due to the presence of the heavy disc, we have been able to enhance the ratio of the moment of inertia of the wheel over the product of the mass of the wheel and the square of the radius of the axle in the range between 9 and 269. In case of pure rolling this is the ratio of the rotational energy over the translational energy. We have studied the rolling motion of the Maxwell wheel with cylindrical sleeves on the soft surface as a function of this energy ratio. From the deceleration of the wheel we determine the offset distance and the coefficient of rolling friction.

2. Theory

2.1. Coefficient of rolling friction

As the axle rolls along the horizontal track, it brings about a deformation of the soft surface. A resistive force of reaction of the surface acts on the rolling object in the region of contact. As discussed by Tabor [6], in the case of elastic deformation, hysteresis contributes a major part to the loss of energy. Witters and Duymelinck [7] have presented a model of the resistive force on the basis of which they have determined the coefficient of rolling friction from the deceleration of the rolling object.

In figure 1 we show a simplified picture of the model which gives the effect of the forces acting in the contact region [8–10]. The net reaction of the contact surface acts at a point Q which is shifted by a distance ρ in the horizontal direction of motion from the point P. QR is the direction in which the reaction force of the deformed surface acts. F is the total horizontal component of this force acting on the axle on the two sides of the disc, placed symmetrically between the tracks. Similarly, N is the total normal reaction though they have been shown to

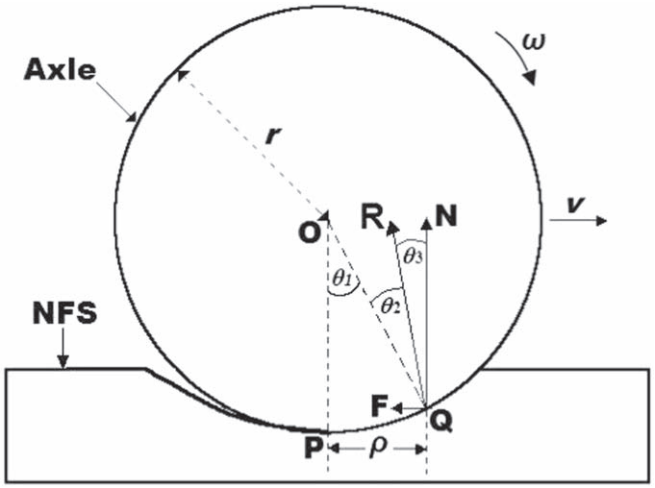

Figure 1. Schematic of the cross section of the axle rolling on a nitrile foam sheet (NFS).

act on one surface for simplicity. mg is the total weight of the wheel which has been shown in figure 1 to act vertically downward through the center O of the axle along OP. We write the equations that govern the motion of the wheel as

$$ma = -F, \tag{1}$$

$$N - mg = 0, \tag{2}$$

and the torque of the forces about the center of the axle is written as

$$\tau = Fr - \rho N = I\frac{a}{r}. \tag{3}$$

Here a is the acceleration and I is the moment of inertia of the wheel about an axis through its centre of mass and parallel to the length of the axle. The radius of the axle is r. In equation (3) the torque of the force F has been written as Fr in the first approximation. This is valid, as the offset distance ρ turns out to be very small compared to the radius of the axle. Eliminating the term F between these equations we get the expression for the acceleration given by

$$a = -g\frac{\frac{\rho}{r}}{1 + k}, \tag{4}$$

where

$$k = \frac{I}{mr^2} = \frac{4I}{md^2}, \tag{5}$$

where d is the diameter of the axle. For pure rolling the dimensionless variable k is the ratio of the rotational energy of the wheel over its translational energy and is a positive quantity. We find from equation (4) that the acceleration is a negative quantity. So physically we get a decelerated motion. By measuring the deceleration we determine $\frac{\rho}{r}$. We can perform a similar analysis to eliminate the acceleration from equations (1) to (3) and get an expression for F. It is easy to show

$$F = \frac{\rho}{r}\left(\frac{1}{1+k}\right)mg. \tag{6}$$

We define the coefficient of rolling friction as

$$\mu_R = \frac{F}{mg} = \frac{\rho}{r}\left(\frac{1}{1+k}\right). \tag{7}$$

As has been explained by Weltner [11] in his reference section, the coefficient of rolling friction according to Witters and Duymelinck [7] is the angle θ_1 as shown in figure 1 of the present work. In the small angle limit this is approximately equal to $\frac{\rho}{r}$, whereas, according to our definition it is approximately equal to the angle θ_3.

We can adjust the initial release position of the wheel on the inclined plane so that the wheel comes to rest at a suitable position on the horizontal track.The distance from the starting position on the horizontal plane to the stopping position is d_s which we measure experimentally. We will check later on how the total energy lost over a distance d_s matches the total initial energy of the wheel. The total initial energy is

$$E_i = \frac{1}{2}mu^2(1+k), \tag{8}$$

where u is the initial linear velocity of the wheel at a fixed position on the horizontal part of the track.

2.2. Energy loss

An elemental energy loss by the wheel due to work done as a result of a rotation of the axle by a small angle $\mathrm{d}\phi$ is given by

$$\mathrm{d}E_L = F\mathrm{d}s - \tau\mathrm{d}\phi, \tag{9}$$

where $\mathrm{d}s = r\mathrm{d}\phi$ for pure rolling. From equations (3) and (2) we get

$$\mathrm{d}E_L = F\mathrm{d}s - (Fr - \rho N)\mathrm{d}\phi \tag{10}$$

which gives

$$\mathrm{d}E_L = \rho mg\mathrm{d}\phi, \tag{11}$$

where $N = mg$ from equation (2). We find that the net work done by the frictional force F is zero as a result of the constraining relation of pure rolling [12]. The force F does not do any net work. The force opposes the linear motion and at the same time provides the torque which facilitates rolling. The entire energy is lost because of the torque produced by the vertical component N.

From figure 1 we find that the reaction of the soft surface when the hard object is rolling on it is along QR which is not directed towards the center of the wheel. This is because of the asymmetry between the forward compression force on the soft surface and the force at release at the back [8, 13]. As a result of this asymmetry there is hysteresis and resulting loss of energy. We find μ_R which is approximately equal to the angle θ_3 in figure 1 is less than $\frac{\rho}{r}$ which is approximately equal to the angle θ_1. This is consistent with the definition of μ_R given by equation (7) where μ_R is less than $\frac{\rho}{r}$ by a factor of $(1+k)$.

Integrating equation (11) we get

$$E_L = \frac{\rho}{r}mgd_s \tag{12}$$

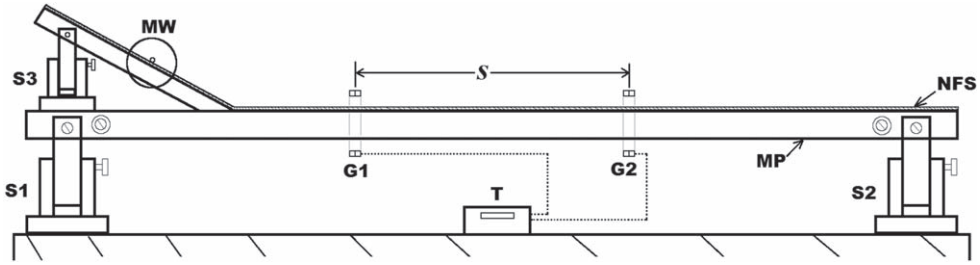

Figure 2. Schematic of the experimental setup.

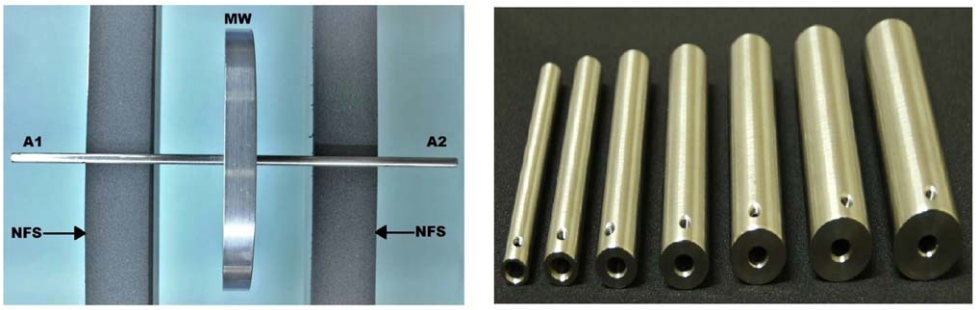

Figure 3. Photograph of (a) the top view of the wheel placed on the NFS; (b) a set of 7 sleeves.

and hence

$$\frac{\rho}{r} = \frac{E_L}{mgd_s}. \tag{13}$$

We find that $\frac{\rho}{r}$ is the energy loss of the system per unit distance of travel per unit load.

3. Experimental setup

The experimental setup designed for this investigation consists of a Maxwell's Wheel (MW), rolling plane arrangement and a digital timer (T) with two photogates (G1 and G2) as illustrated in figure 2.

The Maxwell's wheel was fabricated by fine machining and fitting an aluminum disc with a solid stainless steel rod as its axle. The diameter of the disc was 120 mm and its thickness was 12 mm. The diameter of the axle was 4.96 mm and its length 310 mm. The rolling plane was fabricated using two identical heavy metal pipes (MP) with square (30×30 mm) cross section. The two pipes were machined to make them straight and coupled at their ends as parallel tracks using two identical metal spacers. The gap between the two tracks was 75 mm. This complete rolling plane was mounted on a table so that the disc could rotate freely between the tracks without touching the table. The track was levelled horizontally using two stands S1 and S2 and a digital inclinometer. Long strips of nitrile foam sheet (NFS) 30 mm wide and 6 mm thick were pasted on each track.

The top view of the wheel placed on the NFS is shown in figure 3(a). Figure 3(b) shows the cylindrical stainless steel sleeves which could be fitted on the axle. By changing the sleeves we could vary the diameter of the axle from 4.96 to 20.00 mm.

An adjustable inclined plane was fabricated and coupled to the horizontal plane using the stand S3 as shown in figure 2, to provide initial velocity to the wheel. The region of joining of the two planes was smoothened by extending and pasting the nitrile foam sheet on the inclined plane.

A digital smart timer (T) was used with two narrow beam IR photogates (G1 and G2) for the measurement of the time interval. The timer (PASCO ME-8930) was used in the two gate mode by which the time interval between the wheel's axle crossing the first gate and the second gate was measured.

4. Data collection

The nitrile foam sheet has been chosen carefully so that the foam does not undergo too much plastic deformation. Before final data collection, the foam was subjected to repeated traversals by the rolling wheel with the pair of sleeves with maximum weight. This was done to bring the foam to an elastic equilibrium state. After about 200 traversals the foam was found to have reached an equilibrium. This was checked by calculating the offset distance ρ by measuring the deceleration of the wheel. Initially we saw a gradual decrease of ρ until it settled for a steady value within experimental uncertainty in repeated measurements. Under this condition the final data was recorded. The wheel was carefully aligned so that its disc was placed symmetrically between the tracks. It was released from the inclined plane and made to roll first on the inclined part and then on the horizontal section. For a given diameter of the sleeve the initial position of release was kept fixed in repeated measurements so that the initial energy measured at the first photogate was fixed. The initial position of release of the wheel was decided by looking at the stopping position which we adjusted to a little beyond the 90 cm mark for each sleeve. The release position for each sleeve on the inclined track was different.

The first photogate (G1) was kept fixed at the 35.0 cm mark on a meter scale which was fixed by the side of the metal pipe (MP). The second photogate (G2) was clamped at 50.0 cm for the first reading. The distance betwen the photogates was s as shown in figure 2. The wheel was allowed to roll down the inclined plane from a fixed point.The time interval t for the axle to pass between gates G1 and G2 was noted. This measurement of t was repeated three times by releasing the wheel from exactly the same position on the inclined track. G2 was then clamped successively at 55.0 cm, 60.0 cm upto 90.0 cm at an interval of 5.0 cm. The time interval for the wheel to pass between the two gates was noted for each position of G2. The process was repeated for all the sleeves. The whole process of data collection was repeated two more times. For each distance s from G1 for each sleeve, we had a total of nine measurements of time. A set of data of distances s and average time t was obtained. The position at which the wheel stopped was noted every time and the average stopping distance d_s was determined.

5. Data analysis and results

5.1. Discussions on the coefficient of rolling friction μ_R

In table 1 we have presented the values of the parameters d, m and I of the wheel with various pairs of sleeves attached to the axle. In the last column we give the energy ratio $k\left(=\frac{4I}{md^2}\right)$. We

Table 1. Parameters of the Maxwell's wheel with diameter of the axle without/with sleeves.

Diameter d (m) $\times 10^3$	m (kg)	I (kg m^2) $\times 10^4$	$k = \frac{4I}{md^2}$
4.96	0.3973	6.570	269
8.04	0.4300	6.574	94.6
10.02	0.4609	6.580	56.9
12.02	0.4993	6.592	36.6
13.98	0.5444	6.611	24.8
15.97	0.5942	6.639	17.5
18.04	0.6528	6.682	12.6
20.00	0.7205	6.742	9.36

Table 2. A typical set of data of distance travelled by the wheel and average time taken.

Position of the second photogate G2 (m)	Average time of travel t (s)	Distance of travel s (m)	$\frac{s}{t}$ (m s^{-1})	Average stopping distance (d_s) (m)
0.500	0.832 ± 0.003	0.150	0.180 ± 0.002	
0.550	1.144 ± 0.003	0.200	0.175 ± 0.001	
0.600	1.478 ± 0.002	0.250	0.169 ± 0.001	
0.650	1.861 ± 0.009	0.300	0.161 ± 0.001	
0.700	2.24 ± 0.01	0.350	0.156 ± 0.001	0.576
0.750	2.69 ± 0.01	0.400	0.149 ± 0.001	
0.800	3.21 ± 0.01	0.450	0.140 ± 0.001	
0.850	3.85 ± 0.02	0.500	0.130 ± 0.001	
0.900	4.74 ± 0.04	0.550	0.116 ± 0.001	

Diameter of the sleeve $d = 20.00 \times 10^{-3}$ m.
Position of the first photogate G1: 0.350 m.
Average stopping position of the wheel: 0.926 m.

have already seen in the theory section that k is the ratio of the rotational energy over the translational energy. We find that k goes on decreasing with the increasing diameter d of the sleeves. The reason for this is the fact that the central disc of the wheel contributes the largest part of the rotational energy. When we add the sleeves, the proportional increase in the rotational energy is less than the proportional increase of the translational energy.

In section 4 we have described our method of collecting data. One typical set of data for the distance travelled by the wheel and the corresponding average time taken has been shown in table 2 for the pair of sleeves of diameter 20.00 mm. If an object moves by a distance s in time t with constant deceleration a, we have the relation

$$s = ut - \frac{1}{2}at^2, \tag{14}$$

where u is the initial velocity. From this we get

$$\frac{s}{t} = u - \frac{1}{2}at. \tag{15}$$

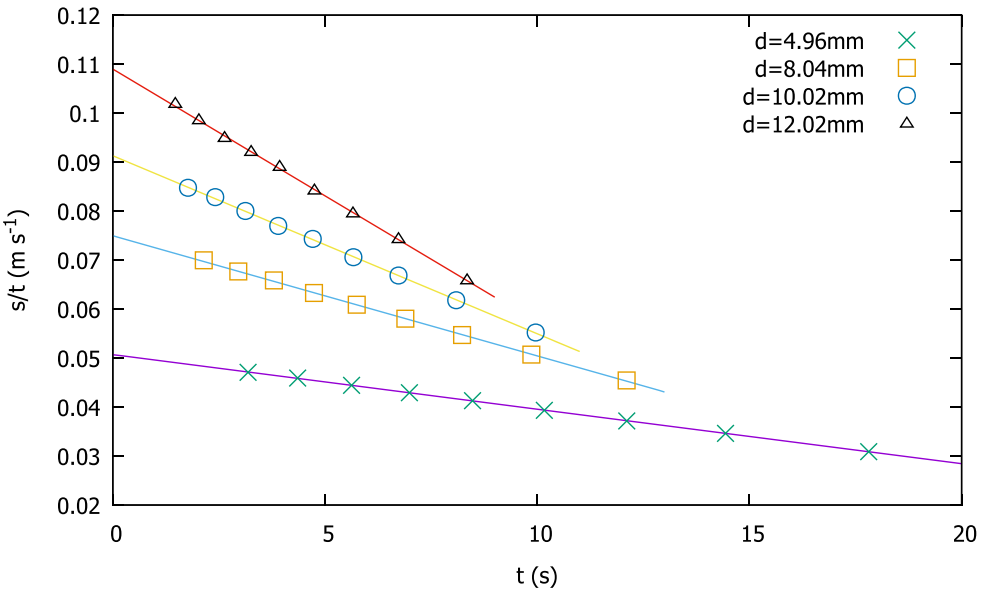

Figure 4. A plot of $\frac{s}{t}$ as a function of t for four diameters d of the sleeves.

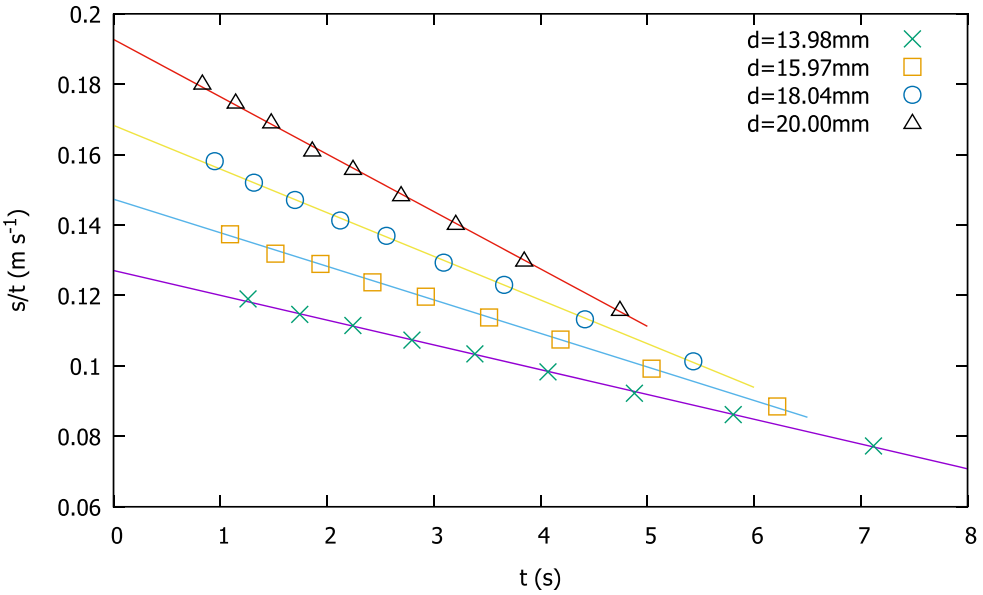

Figure 5. A plot of $\frac{s}{t}$ as a function of t for sleeves of larger diameters.

We have plotted $\frac{s}{t}$ as a function of t for all values of diameters d of the sleeves as shown in figures 4 and 5. The data points for all the sleeves can be found to fall on straight lines. This clearly indicates that the wheel's deceleration is constant.

Table 3. Offset distance and the coefficient of rolling friction against the diameter of the axle.

Diameter d(m) $\times 10^3$	Deceleration a (m s^{-2}) $\times 10^3$	$\frac{\rho}{r} \times 10^3$	Offset distance ρ(m) $\times 10^3$	$\mu_R \times 10^3$
4.96	2.23 ± 0.02	61.3 ± 0.7	0.152 ± 0.002	0.227 ± 0.003
8.04	4.91 ± 0.07	47.9 ± 0.7	0.192 ± 0.003	0.501 ± 0.007
10.02	7.3 ± 0.1	42.9 ± 0.7	0.215 ± 0.004	0.74 ± 0.01
12.02	10.3 ± 0.2	39.7 ± 0.6	0.238 ± 0.004	1.06 ± 0.02
13.98	14.1 ± 0.3	37.1 ± 0.7	0.259 ± 0.005	1.44 ± 0.03
15.97	19.1 ± 0.4	36.0 ± 0.7	0.287 ± 0.005	1.94 ± 0.04
18.04	24.8 ± 0.6	34.4 ± 0.8	0.310 ± 0.007	2.53 ± 0.06
20.00	32.6 ± 0.6	34.4 ± 0.6	0.344 ± 0.006	3.32 ± 0.06

Uncertainty in the mean time was calculated from the dispersion of the nine measurements of time. Uncertainty for the position of photogates G1 and G2 was set at 1.0 mm each. Uncertainties in $\frac{s}{t}$ were determined by propagating the uncertainties in s and t. Chi squared minimised linear fit [14] was done on $\frac{s}{t}$ as a function of t. The fitted lines are shown on the data points. The magnitudes of the slopes give half of the deceleration a, experienced by the wheel for different sleeves. In table 3 we have shown the decelerations for the wheel with different sleeves with their uncertainties. The initial velocity u is also determined from the fit. The values of different initial velocities with their uncertainties are shown in table 4. The uncertainties in these two variables a and u, have been estimated by the method given for linear fit by Burrel [15].

From these decelerations we determine the ratio $\frac{\rho}{r}$ using equation (4) and hence ρ for different values of r. We find the offset distances ρ lie between 0.152 and 0.344 mm with the values increasing from a lower diameter to a higher diameter. The uncertainties in this variable are found to be less than or around 2%. In the last column of table 3 we show the values of the coefficient of rolling friction μ_R estimated from equation (7).

In figure 6 we have plotted μ_R as a function of k. In section 5.2 we have explained why μ_R increases with decreasing k the way it does. It implies that the less the rotational energy compared to the translational energy, the more the coefficient of rolling friction, at least for horizontal motion. On the other hand, this also means that more the rotational energy compared to the translational energy, the less the coefficient of rolling friction. Since μ_R and k are both dimensionless, we plot them in log–log scale. In figure 7 we plot log μ_R with its uncertainties against log k. We see an approximate linear feature of the plot. In the first approximation we fit a linear function of the form

$$\log\mu_R = c - b \times \log k. \tag{16}$$

A chi squared minimisation procedure gives the values $c = -1.73 \pm 0.02$ and $b = 0.79 \pm 0.01$. This leads to a power law of the form

$$\mu_R = pk^{-b} \tag{17}$$

with $p = 0.0186 \pm 0.0004$. The fitted line has been shown on the data points. We find a fairly good fit within experimental uncertainties. The fitted values of p and b depend on the

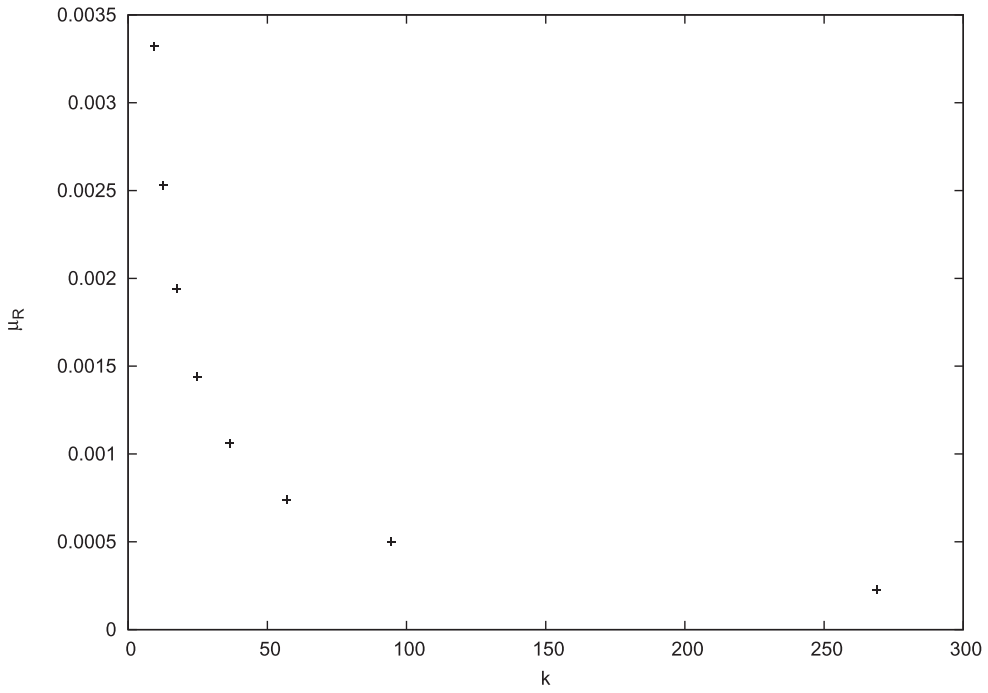

Figure 6. A plot of μ_R as a function of k.

Table 4. Energy loss in the rolling motion.

Diameter d (m) $\times 10^3$	Initial velocity u (m s^{-1}) $\times 10^3$	Initial energy (J)	Stopping distance (d_s) (m)	Energy loss per unit distance (J m^{-1})	Total energy loss (J)
4.96	50.7 ± 0.2	0.138 ± 0.001	0.579	0.239 ± 0.003	0.138 ± 0.002
8.04	75.0 ± 0.3	0.116 ± 0.001	0.575	0.202 ± 0.003	0.116 ± 0.002
10.02	91.3 ± 0.4	0.111 ± 0.001	0.576	0.194 ± 0.003	0.112 ± 0.002
12.02	109.0 ± 0.4	0.111 ± 0.001	0.578	0.194 ± 0.003	0.112 ± 0.002
13.98	127.1 ± 0.6	0.113 ± 0.001	0.575	0.198 ± 0.004	0.114 ± 0.002
15.97	147.3 ± 0.8	0.119 ± 0.001	0.576	0.209 ± 0.004	0.120 ± 0.002
18.04	168 ± 1	0.125 ± 0.002	0.574	0.220 ± 0.005	0.126 ± 0.003
20.00	192.7 ± 0.9	0.139 ± 0.001	0.576	0.243 ± 0.004	0.140 ± 0.002

nature of the pair of surfaces in contact. From table 3 we find that μ_R increases with the radius of the sleeves and the corresponding increase in the mass and the moment of inertia of the wheel. The power law represents our data as plotted in figure 6 in a compact form. It is the nature of our data shown in figure 6, expressed in terms of two dimensionless variables that has led to the power law. In the next approximation a nonlinear fitting was done. However, the results of the fitted parameters comparable to those of the linear fit, differ very little.

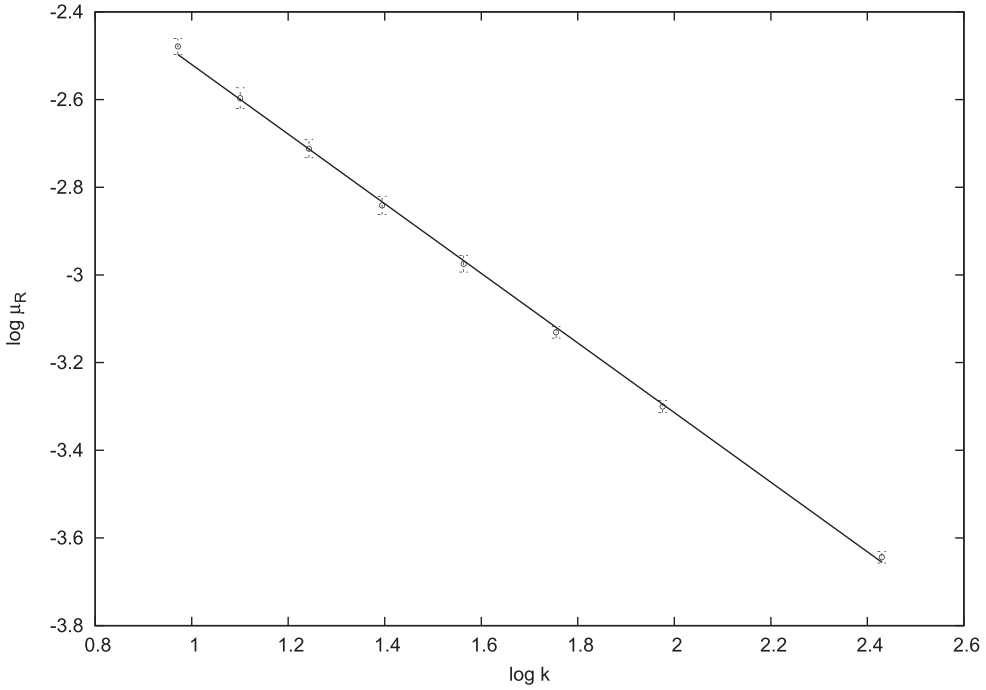

Figure 7. A plot of log μ_R versus log k with the linear fit.

5.2. Discussions on the offset distance ρ

As discussed in the beginning of section 2.1, A wheel rolling along a soft surface brings about deformation on it. The more the radius of the sleeves and the mass of the wheel, the larger is the deformation over a larger area of contact between the sleeves and the surface. As a result ρ increases. However, as explained in the beginning of section 5.1, k decreases with increasing r and m. So, we have ρ increasing with decreasing k as the data show in tables 1 and 3.

In figure 8 we have plotted $\frac{\rho}{r}$ as a function of the energy ratio k. As the radius of the sleeves increase, the rate of increase of ρ is less than the rate of increase of r as can be found from table 3. So, $\frac{\rho}{r}$ decreases with increasing r and m and consequently decreases with decreasing k as can be seen from figure 8. From tables 1 and 3 we find that while k decreases by about 95% on the average between the highest and lowest values, $\frac{\rho}{r}$ decreases by only about 45%. This explains why μ_R as defined in equation (7), increases with decreasing k with a faster rate at lower values of k. If we plot $\frac{\rho}{r}$ against k in log–log scale, it shows signs of nonlinearity towards the lowest values of k. So we do not consider this as the coefficient of rolling friction as has been done in [7].

From equations (7) and (17) we find

$$\frac{\rho}{r} = \mu_R(1 + k) = pk^{-b}(1 + k). \tag{18}$$

This shows that $\frac{\rho}{r}$ is also a function of k. From equation (18) we get

$$\rho = pk^{-b}(1 + k)r. \tag{19}$$

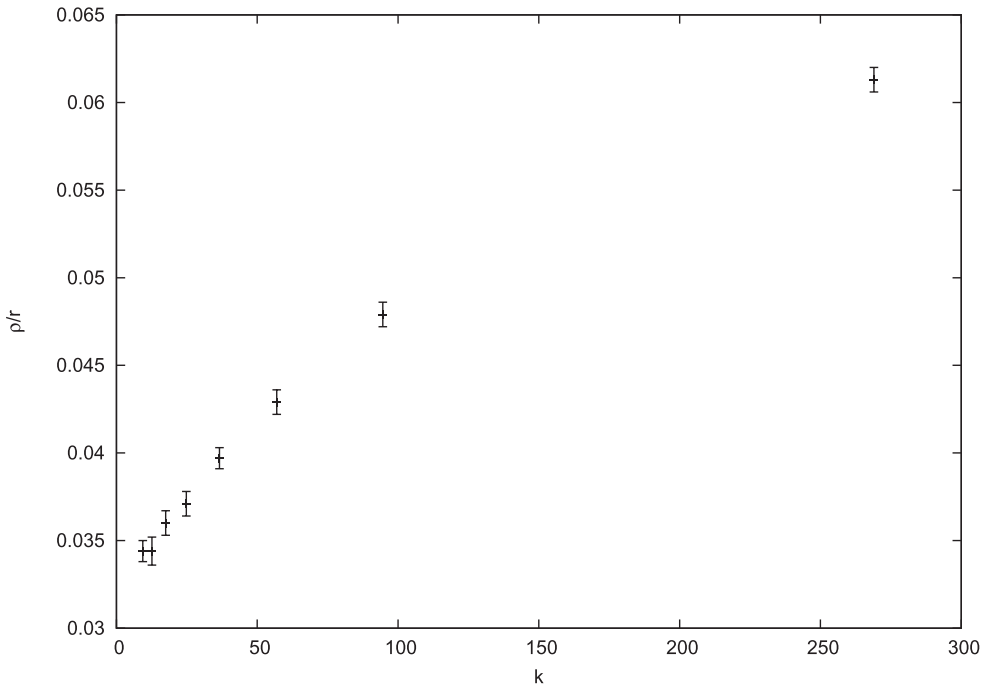

Figure 8. A plot of $\frac{\rho}{r}$ as a function of k.

This is the analytic expression for the offset distance as a function of the radius of the sleeves and the energy ratio k of the wheel. From equation (18) we expect $\frac{\rho}{r}$ to be constant for a fixed k for objects of same material but of different dimensions rolling on a given surface.

5.3. Discussions on the energy loss

Initial energy of the wheel E_i is calculated using equation (8). In table 4 we have presented the diameters of the sleeves along with the distances (d_s) travelled by the wheel before they come to rest and their initial energies. Using equation (12) we calculate the total energy loss as the wheel comes to a stop. We can see that this energy loss and the total initial energy match very well within experimental uncertainties which are less than or around 2%. Since the measurements of d_s are independent of the measurements of s and t which give the initial velocity and the deceleration, this matching shows that our measurements are fairly accurate.

From equations (13) and (18) we find

$$\frac{E_L}{d_s} = \frac{\rho}{r}mg = \mu_R(1 + k)mg. \tag{20}$$

From table 4 we find that as the diameter of the sleeves increase, energy loss per unit distance initially decreases and then after reaching a minimum starts increasing. This can be explained with equation (20). We know that with increasing radius, $\frac{\rho}{r}$ decreases. So initially we see a decrease in the energy loss. However, with increasing r, mg also increases and as a result, energy loss per unit distance starts increasing after hitting a minimum. In our experiment, minimum energy loss occurs at 10.0–12.0 mm diameter of the sleeves corresponding to k values ranging from about 57 to 37 as can be found from tables 4 and 1. We find that a proper

choice of the energy ratio and the load can lead to minimising the energy loss of a wheel rolling on a given surface.

Further, we find from equation (20) that the energy loss over a distance travelled by the wheel is proportional to the load for a fixed energy ratio k in the first approximation. The same conclusion was arrived at by Tabor [6]. Very recently Minkin and Sikes [16] have reported a simple method for the determination of the coefficient of rolling friction from the loss of energy.

6. Summary and conclusions

We have carried out an experimental investigation where we allow a Maxwell's wheel to acquire some initial energy and then roll along a pair of horizontal tracks until it comes to a stop. The cylindrical axle of the wheel runs on a soft nitrile foam sheet on the two sides of the disc which rotates in the air. A unique feature of our experimental setup is that we can vary the ratio of the rotational over the translational energy of the wheel by attaching a pair of sleeves on the two sides of the axle. We have determined the offset distance and the coefficient of rolling friction accurately as a function of the energy ratio. We find that the coefficient follows a power law as a function of the energy ratio in the first approximation. As far as we are aware, this functional relationship has not been reported so far in the relevant literature. It follows from this that if the energy ratio is kept fixed, the offset distances increase linearly with the radius. The coefficient of rolling friction as defined by us, decreases as the rotational energy increases more in comparison to the translational energy of the wheel. Offset distances increase with the increasing radius of the sleeves.

We have shown that the offset distance is related to the energy loss of the system. By noting the distances over which the wheels come to rest, we show that the total loss of energy is the same as the total initial energy within experimental uncertainty which is less than or around 2%. This gives us a check on the accuracy of the offset distances determined. The loss of energy per unit distance is found to be proportional to the load if the energy ratio remains constant. However, if the energy ratio and load are varied, the energy loss per unit distance is found to pass through a region of minimum values for a small range of the energy ratio.

Acknowledgments

We acknowledge the support of the Govt. Of India, Department of Atomic Energy, under the National Initiative on Undergraduate Science of HBCSE-TIFR (Project No. 12-R and D-TFR-6.04-0600). SC would like to thank Prof A K Mallik for helpful discussions.

ORCID iDs

Surajit Chakrabarti https://orcid.org/0000-0002-7478-2282

References

[1] Domenech A, Domenech T and Cebrian J 1987 Introduction to the study of rolling friction *Am. J. Phys.* **55** 231–5
[2] Alaci S, Cerlinca D A, Ciornei F C, Filote C and Frunza G 2015 Experimental highlight of hysteresis phenomenon in rolling contact *J. Phys.: Conf. Ser.* **585** 012010
[3] Cross R 2019 Energy losses in a rolling ball *Eur. J. Phys.* **40** 035003

[4] ScienceFirst 2020 Maxwell's Wheel https://shop.sciencefirst.com/rotationoscillation/2511-maxwell-s-wheel.html
[5] www.superlon.com.my
[6] Tabor D 1955 The mechanism of rolling friction II. The elastic range *Proc. Roy. Soc.* A **229** 198–220
[7] Witters J and Duymelinck D 1986 Rolling and sliding resistive forces on balls moving on a flat surface *Am J. Phys.* **54** 80–3
[8] Hierrezuelo J and Carnero C 1995 Sliding and rolling: the physics of a rolling ball *Phys. Educ.* **30** 177–81
[9] Cross R 2016 Coulomb's law for rolling friction *Am J. Phys.* **84** 221–30
[10] Vozdecky L, Bartos J and Musilova J 2014 *Eur. J. Phys.* **35** 055004
[11] Weltner K 1987 Central drift of freely moving balls on rotating disks: a new method to measure co-efficients of rolling friction *Am J. Phys.* **55** 937–42
[12] Carnero C, Aguiar J and Hierrezuelo J 1993 The work of the frictional force in rolling motion *Phys. Educ.* **28** 225–7
[13] Cross R 2017 Origins of rolling friction *Phys. Educ.* **52** 055001 (4pp)
[14] Bevington P R and Keith Robinson D 2003 *Data Reduction and Error Analysis for the Physical Sciences* 3rd edn (New York: McGraw-Hill) pp 104–5
[15] Burrell K H 1990 Error analysis for parameters determined in nonlinear least-squares fits *Am J. Phys.* **58** 160–4
[16] Minkin L and Sikes D 2018 Coefficient of rolling-friction lab experiment *Am J. Phys.* **86** 77–8 Notes and discussion